

## INTEGRATED ANALYSIS OF INHOMOGENEOUS STRUCTURAL MONITORING DATA OF A MONOLITHIC BRIDGE

Werner Lienhart  
Graz University of Technology, Austria

Fritz K. Brunner  
Graz University of Technology, Austria

### Abstract

In structural monitoring geodetic sensors (tacheometers, GPS, ...) are commonly used in combination with other sensors, like level sensors or fiber optic sensors. The hybrid measurements are inhomogeneously distributed throughout the structure as well as in time. For a detailed understanding of the structural behavior the data from all sensors need to be analyzed. For this purpose, an Integrated Analysis Method (IAM) has been developed using a Finite Element Model (FEM) to combine all measurement data for the deformation analysis. The proposed IAM is applied to the deformation analysis of a monolithic bridge, which was monitored with embedded fiber optic sensors, inclinometer data and geodetic measurements for more than two years.

### MONOLITHIC BRIDGE

To date the widening of alpine roads is mostly done using excavations with retaining walls. However, the construction of retaining walls is expensive and requires substantial earthworks, which adversely affect the sensitive alpine ecological system. In order to overcome these problems, a new bridge construction was developed by the engineering office Eisner (Graz, Austria).

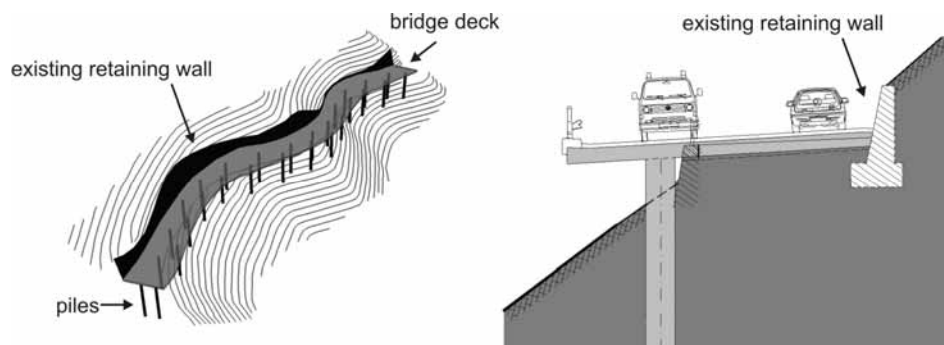


Figure 1: New bridge construction for the widening of roads in steep terrain

A prototype of this new bridge design was built near Schladming (Austria) in 2002, see fig. 1. The concrete deck of the bridge is 150m long and does not contain any expansion joints or bridge bearings. Furthermore, the bridge deck is connected to the existing road without expansion joints. The bridge deck is linked to the slope with 30 concrete piles of about 8m depth. The reinforcement of the piles was extended into the bridge deck, thus generating a monolithic structure. The cross section in fig. 1-right shows that the new deck rests up to 2/3 on the old road. In the central section as well as on both ends the bridge deck rests entirely on the old road. More details about the construction can be found in [1]. This bridge is referred to as Monolithic Bridge in this paper.

Between winter and summer, large temperature differences in the bridge of more than 40K are possible due to the high altitude of 1000m. Such a temperature change would result in a length change of about 7cm if the bridge could expand freely, causing serious problems in the transition regions between bridge and road. However, due to the curved shape of the bridge and the monolithic connection to the piles with smaller movements were expected. Since the detailed behavior of the new bridge construction was unknown, the Institute of Engineering Geodesy and Measurement Systems (EGMS) of Graz University of Technology developed a monitoring scheme for the bridge.

## MEASUREMENT PROGRAM

We proposed to use the SOFO System [2] for measuring internal length changes. The measurement principle of this fiber optic measurement system is based on low-coherence interferometry. Therefore, it is well suited for discontinuous long term monitoring because the zero reference is not lost. SMARTEC, the manufacturer of the SOFO system, specifies a precision of  $2\mu\text{m}$  independent of the sensor length. This precision was verified by investigations in the laboratory of EGMS and on site, [3] and [4].

For the monitoring of the Monolithic Bridge SOFO sensors with a length  $L$  of 5m were chosen. Considering the measurement precision of  $2\mu\text{m}$  and the sensor length of 5m, strain values can be determined with a precision of  $4 \cdot 10^{-7}$ . Due to financial constraints, only three measurement profiles (MP) were selected in the curved sections of the bridge, see fig. 2.

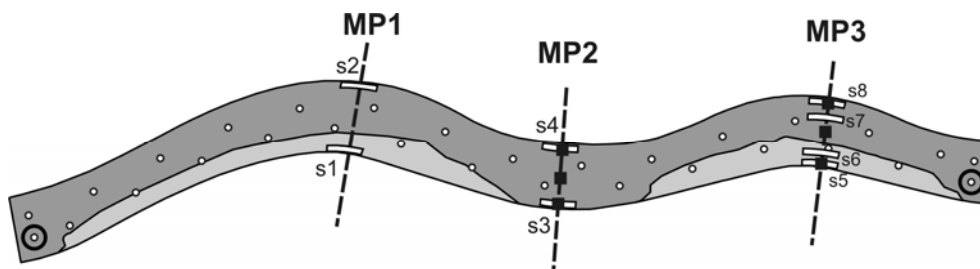


Figure 2: Top view of the Monolithic Bridge with cantilevered (bright grey) and non cantilevered areas (dark grey). Positions of eight SOFO sensors (white) are shown in three measurement profiles (MP), six pairs of resistance temperature sensors (black squares) and two inclinometer tubes (black circles)

The installation of the sensors is critical for their survivability, [5]. We mounted the sensors under the reinforcement bars (fig. 3) where they were held, but not fixed using cable ties. This way pouring the concrete did not cause any problems. In order to separate the temperature effects from the measured strain values, resistance temperature detectors (RTD) were also embedded. Three pairs of platinum RTD sensors were installed in the measurement profiles MP2 and MP3. No temperature sensors were installed in MP1 due to financial constraints. Each pair consists of two vertically separated sensors (fig. 3) to compute vertical and horizontal temperature gradients.

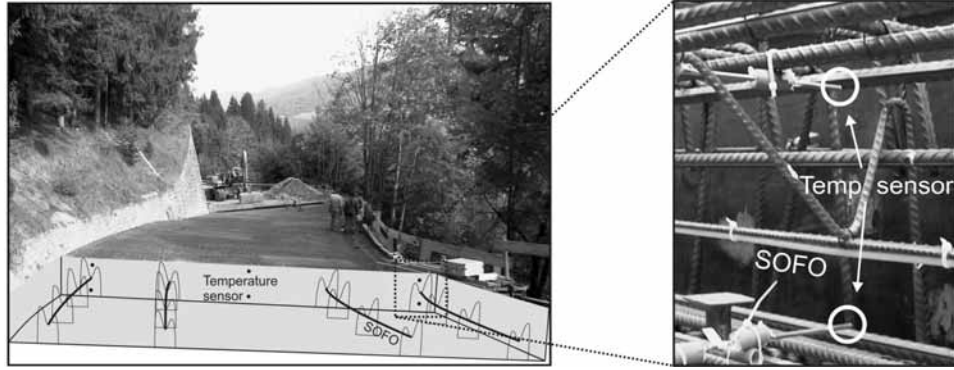


Figure 3: Embedded sensors in measurement profile 3

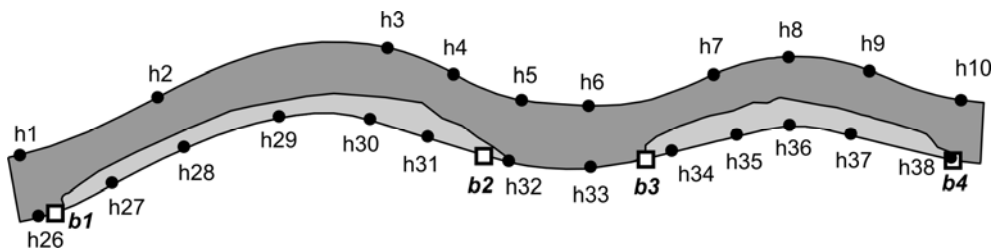


Figure 4: Positions of levelling points (black circles) and four traverse points (white squares)

In addition to the embedded sensors, traditional geodetic techniques were used for monitoring the Monolithic Bridge. Height changes of the concrete deck were determined by precise levelling at more than 20 points. The positions of these points are indicated in fig. 4. To measure the length changes of the entire bridge, four bolts for mounting reflecting targets were installed in the bridge deck, see fig. 4. For the computation of absolute deformations, the geodetic measurements need to be connected to stable reference points, which were established to the west and east of the Monolithic Bridge.

## PRELIMINARY ANALYSIS

The bridge was monitored for more than two years. All sensors were measured in 6 major measurement epochs. Fig. 5 shows the length changes of the SOFO sensors with respect to the first measurement epoch (SOFO s3 was destroyed by construction work before the measurements commenced, and SOFO s7 could not be measured any longer after day 374).

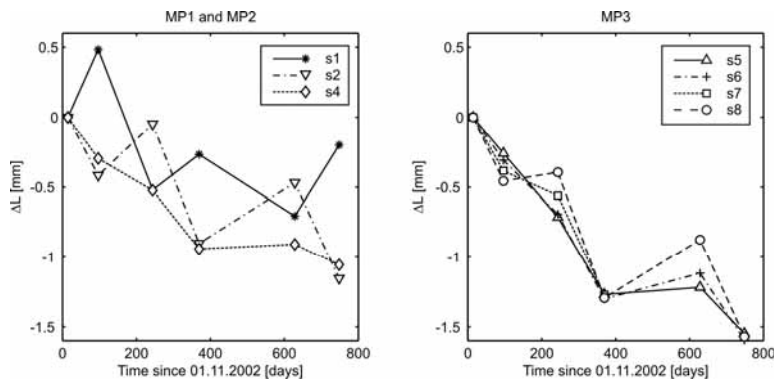


Figure 5: Measured length changes of the SOFO sensors relative to the first epoch

All SOFO sensors of MP3 measured a general shortening of more than 1mm within the first year, fig. 5-right. However, the individual length changes of each sensor cannot be interpreted at this stage by the deformation pattern of the whole Monolithic Bridge, as connection measurements between the sensors were not possible.

In order to identify the cause of the deformations, the measurement object can be considered as a physical object, which transforms forces acting on the structure into deformations, [6]. In a first step, internal temperature changes  $\Delta T_i$  are taken into account as causative forces. In order to convert these forces into deformations (length changes  $\Delta L_i$ ), a functional model of the system behavior could be used

$$\Delta L_i = \alpha \cdot L \cdot \Delta T_i \quad (1)$$

where  $\alpha$  is the expansion coefficient of the structure, and  $L$  is the original length.

In this case all fiber optic measurements are linked by one single parameter, i.e. the thermal expansion coefficient  $\alpha$ . However, such a simple model is not applicable for the whole Monolithic Bridge due to the following reasons:

- The monolithic structure cannot expand freely. Therefore the measured length changes  $\Delta L_i$  are smaller than in unrestricted expansions. As a result the calculated  $\alpha$  value will be different to the thermal expansion coefficient of the material, thus loosing its physical meaning.
- Due to the curved shape of the bridge and the monolithic connection to the piles, different areas of the bridge will react differently to the same temperature change. Thus, it is not possible to use one global regression coefficient for all sensors.

A serious problem occurs in linking the internal strain measurements (SOFO sensors) to the external geodetic measurements as only the latter measurements can be used in the standard deformation analysis, e.g. [7]. Thus, an additional model needs to be used to express the structural deformations as a function of the forces acting on the structure and the material properties. For this purpose we have found the Finite Element Model (FEM) of the structure very useful.

## INTEGRATED ANALYSIS METHOD

Fig. 6 shows a Finite Element Model (FEM) of the bridge. The mountain slope is also part of the FEM and was modeled with two different material layers, which are shown by different shading in fig. 6-right. This was an outcome of the inclinometer measurements, which clearly indicated that the behavior of the slope changed at a depth of about 3m. As a result of the FEM, nodal displacements are obtained. Length changes can be calculated from these nodal displacements and compared with the actual measured deformations using the fiber optical sensors.

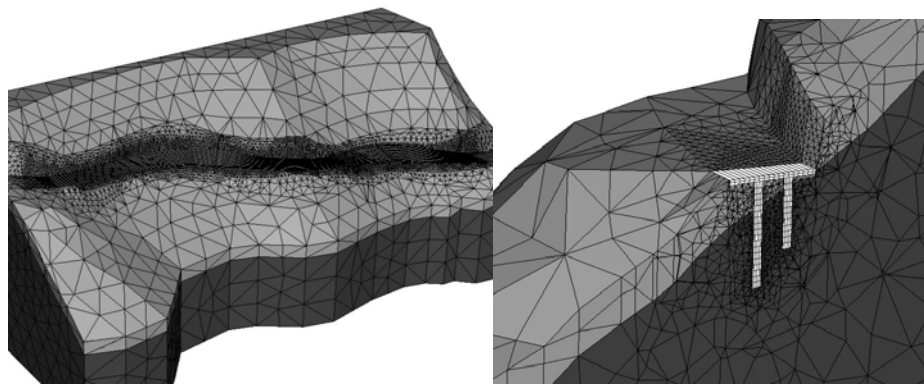


Figure 6: FEM of the Monolithic Bridge and the mountain slope, entire model (left), cut through (right)

In the following we will show how the differences between measured and calculated deformations can be used to estimate the deformations, to gain a calibrated physical model, and to identify areas or times with significant differences, see fig. 7. We call our approach Integrated Analysis Method (IAM) because it enables the seamless analysis of inhomogeneous measurement data taken at different positions and at different times by incorporating a physical model, i.e. the FEM.

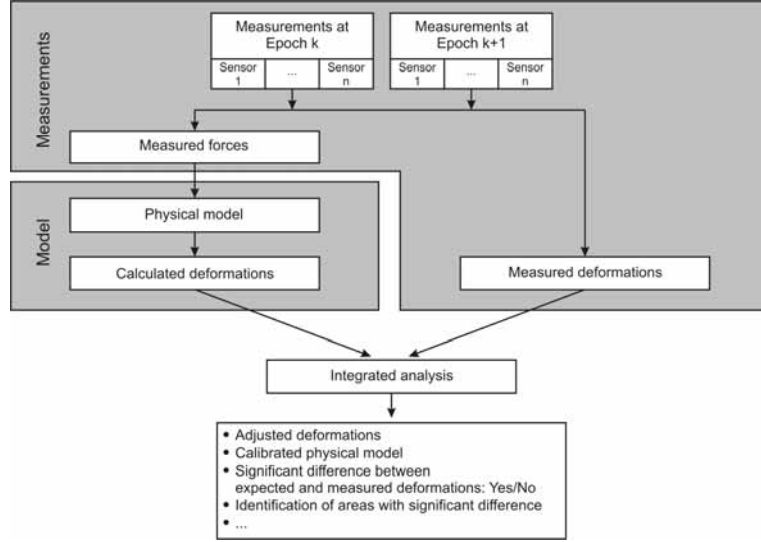


Figure 7: Basic outline of an Integrated Analysis Method

The development of the proposed method is based on [8] and [9]. Here only the basic idea is presented whilst further details can be found in [4].

The method differentiates between a measurement and a system part and also uses the variance co-variance matrices (VCM) of the measurements. The measurement part consists of the measured deformations  $\mathbf{d}_{MEAS}$ , which should be equivalent to the deformations calculated from the nodal displacements  $\mathbf{u}$ . Generally, the unknown parameters of the FEM will cause a difference, which can be used to estimate the parameter values  $\hat{\mathbf{p}}$ . A Gauss Markov model can be introduced which uses the equivalence of the sum of the measured deformations  $\mathbf{d}_{MEAS}$  and the unknown residuals  $\mathbf{e}_{MEAS}$  to the deformations calculated from estimated nodal displacements  $\hat{\mathbf{u}}$  (eq. 2)

Measurement part

$$\mathbf{d}_{MEAS} + \mathbf{e}_{MEAS} = \mathbf{d}_{FEM}(\hat{\mathbf{u}}), \quad \Sigma_{dd,MEAS} \quad (2)$$

System part

$$\mathbf{u}_{SYS} + \mathbf{e}_{SYS} = \hat{\mathbf{u}} - \mathbf{K}(\hat{\mathbf{p}})^{-1} \cdot \hat{\mathbf{f}}, \quad \Sigma_{SYS} \quad (3)$$

$$\mathbf{p} + \mathbf{e}_p = \hat{\mathbf{p}}, \quad \Sigma_{pp} \quad (4)$$

$$\mathbf{f} + \mathbf{e}_f = \hat{\mathbf{f}}, \quad \Sigma_{ff} \quad (5)$$

where  $\Sigma_{ii}$  are the appropriate VCV matrices of the observations. Equation (3) forces the estimated nodal displacements  $\hat{\mathbf{u}}$  to be identical with the calculated nodal displacements using the estimated physical parameters  $\hat{\mathbf{p}}$  and the estimated forces  $\hat{\mathbf{f}}$ . In the system part, the material parameters ( $\mathbf{p}$ ) and forces ( $\mathbf{f}$ ) are included as pseudo observations (eq. 4 and 5). Equation (3) is introduced as a condition by assigning a large weight to it, meaning

$$\Sigma_{SYS} \rightarrow \mathbf{0} \quad (6)$$

The parameters in the model are the nodal displacements  $\mathbf{u}$ , the material parameters  $\mathbf{p}$  and the forces  $\mathbf{f}$ . In order to estimate the parameters by least squares estimation (LSE), the non-linear problem has to be linearized using approximate parameters  $\xi_0$

$$\hat{\xi} = \xi_0 + d\hat{\xi} = \begin{bmatrix} \mathbf{u}_0 + d\hat{\mathbf{u}} \\ \mathbf{p}_0 + d\hat{\mathbf{p}} \\ \mathbf{f}_0 + d\hat{\mathbf{f}} \end{bmatrix} \quad (7)$$

The corrections to the parameters are calculated using standard least squares estimation, e.g. [7]:

$$d\hat{\xi} = (\mathbf{A}^T \Sigma_{yy}^{-1} \mathbf{A})^{-1} \mathbf{A}^T \Sigma_{yy}^{-1} \mathbf{y} \quad (8)$$

We found it practical to use the initial FEM parameter values as approximate values

$$\mathbf{u}_0 = \mathbf{u}_{FEM} \quad (9)$$

$$\mathbf{p}_0 = \mathbf{p}_{FEM} \quad (10)$$

$$\mathbf{f}_0 = \mathbf{f}_{FEM} \quad (11)$$

Then the observation vector has only non-zero entries in the measurement part

$$\mathbf{y} = \begin{bmatrix} \mathbf{d}_{MEAS} - \mathbf{d}_{FEM}(\mathbf{u}_0) \\ \mathbf{0} \\ \mathbf{0} \\ \mathbf{0} \end{bmatrix} = \begin{bmatrix} \delta \\ \mathbf{0} \\ \mathbf{0} \\ \mathbf{0} \end{bmatrix} \quad (12)$$

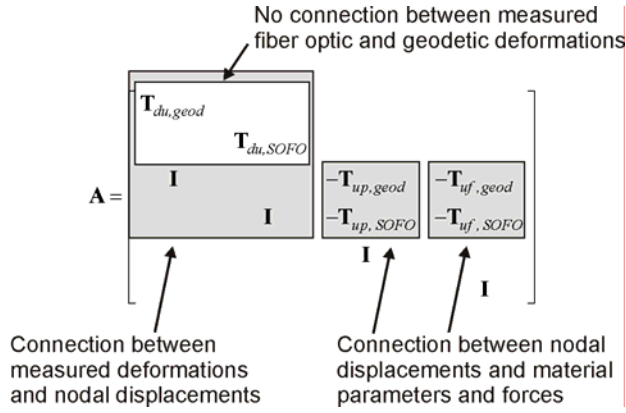
where  $\delta$  is the difference between measured and calculated deformations, which has to be zero after the LSE. The corresponding VCM is given by

$$\Sigma_{yy} = \begin{bmatrix} \Sigma_{dd,MEAS} & & & \\ & \Sigma_{SYS} & & \\ & & \Sigma_{pp} & \\ & & & \Sigma_{ff} \end{bmatrix} \quad (13)$$

where the elements of  $\Sigma_{SYS}$  have to be close to zero in order to generate a condition matrix. The design matrix  $\mathbf{A}$  for the LSE has the following structure

$$\mathbf{A} = \begin{bmatrix} \text{Measurement part} \\ \text{System part} \end{bmatrix} = \begin{bmatrix} \boxed{\frac{\partial \mathbf{d}}{\partial \mathbf{u}}} & & & \\ \mathbf{I} & -\frac{\partial \mathbf{u}}{\partial \mathbf{p}} & -\frac{\partial \mathbf{u}}{\partial \mathbf{f}} & \\ & \mathbf{I} & & \end{bmatrix} = \begin{bmatrix} \boxed{\mathbf{T}_{du}} & & & \\ \mathbf{I} & -\mathbf{T}_{up} & -\mathbf{T}_{uf} & \\ & \mathbf{I} & & \end{bmatrix} \quad (14)$$

where  $\mathbf{I}$  is the identity matrix. The connection between the measurements and the calculated displacements is established by block a). This block contains the partial derivatives  $\mathbf{T}_{du}$  of the deformations with respect to the nodal displacements. The connection between the displacements, the material parameters and the forces is established by block b), which contains the partial derivatives of the nodal displacements with respect to the parameters ( $\mathbf{T}_{up}$ ) and the forces ( $\mathbf{T}_{uf}$ ). The individual points of the FEM are linked together by the off diagonal elements of  $\mathbf{A}$ . In the case of the Monolithic Bridge functional relations are established between previously unconnected sensors. Therefore, the individual fiber optic sensors can now be linked together. Furthermore, connections between the fiber optic sensors and other observation points can be established. This is shown in detail in eq. 15 where the common physical parameters link all nodal points and thus all sensors together.



(15)

## RESULTS

The above presented IAM is now applied to the monitoring data of the Monolithic Bridge. Modeling parameters are the thermal expansion coefficient  $\alpha$  of concrete and Young's moduli of concrete and the two slope layers. The presented results were derived from two measurement epochs with a time difference of 255 days. The results of the IAM using all measurement epochs are given in [4].

**Table 1:** A priori und a posteriori material parameters

Parameter	Initial value		Result of the IAM	
	Value	std	Value	std
$\alpha$ [ppm/K]	10.0	1.0	11.9	0.09
$E_{\text{Concrete}}$ [GN/m <sup>2</sup> ]	30.0	9.0	35.8	0.69
$E_{\text{Slope, upper layer}}$ [GN/m <sup>2</sup> ]	0.10	0.08	0.05	0.005
$E_{\text{Slope, lower layer}}$ [GN/m <sup>2</sup> ]	1.0	0.8	2.1	0.03

The initial values and their assumed standard deviations (std) as well as the values obtained from the IAM are summarized in tab. 1. The results show, for example, that the upper soil layer was initially assumed far too stiff. Its calibrated value is about 50% lower than the initial value.

Fig. 8 shows the calculated and measured displacements of the geodetic points. During the two measurement epochs the internal bridge temperature increased by 15K. In case of unrestricted movements the bridge would expand by 27mm, which could cause problems at the transition regions between bridge deck and road. However, due to the curved shape and the monolithic connection to the 30 piles the bridge deck expanded only by about 8mm, which confirms the valid absence of expansion joints. The calculated displacements agree with the measured displacements to better than 0.5mm. The difference between the measured and calculated (calibrated FEM) displacements are statistically not significant based on the measurement precision. The results of the height changes can be found in [4].

The length changes of the fiber optic sensors (SOFO) are displayed in fig. 9-left. The sensors s7, s8 and s2 (see fig. 2) were not used in the integrated analysis due to reasons explained in [4]. The calculated length changes using the calibrated FEM are in much better agreement with the measured values than the results of the initial model.

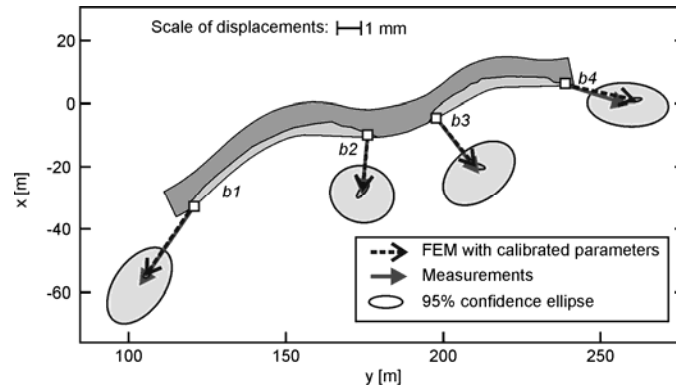


Figure 8: Calculated and measured horizontal displacements of geodetic points

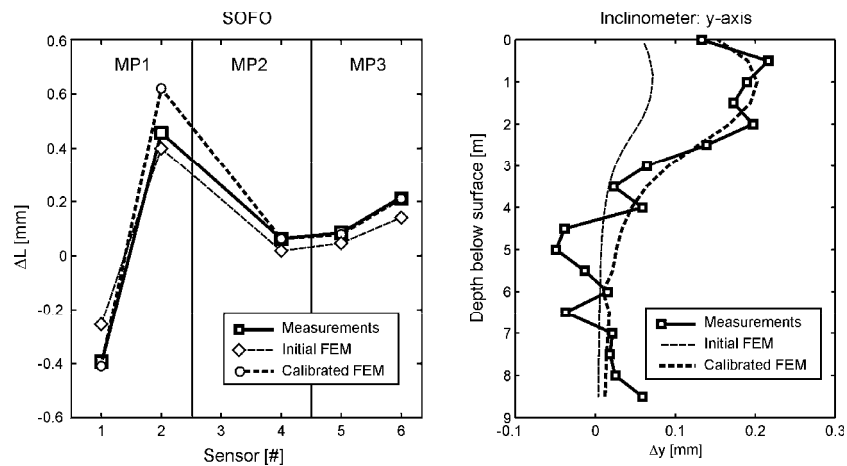


Figure 9: Comparison of calculated and measured deformations for the SOFO sensors (left) and inclinometer results (right)

Fig. 9-right shows that the calibrated material parameters also improved the calculated pile deformations. The calculated deformations fit now closely to the measured deformations, especially in the upper part of the pile.

With the calibrated model it is now possible to calculate deformations for all other measurement epochs and compare them with the measured deformations. If the calibrated model is correct and constant over time, and no other forces than the modeled forces (here temperature changes) are present, then the calculated deformations should be identical to the measured deformations. Using the leveling results the IAM revealed that the height changes along the front edge of the bridge were caused by temperature changes and settlements due to the dead weight of the unsupported part of the bridge deck. However, the full analysis [4] of the monitoring data shows that also deformations independent of internal temperature changes occurred. Because of the high complexity of the Monolithic Bridge and the small number of observation points and measurement epochs it was not possible to verify all reasons for the temperature independent deformations. More bridge piles and also the mountain slope should have been equipped with inclinometer tubes to monitor slope movements.

## CONCLUSIONS

With the proposed IAM it was possible to connect spatially distributed measurements of different types. For the first time internal deformation measurements were analyzed together with external measurements. This is especially important, as no connection measurements can be made. The results of the calibrated FEM are in good agreement

with the measured deformations. The presented method is generic and can be applied to inhomogeneous measurements of any structure. As an example, results of the analysis of the monitoring of a monolithic bridge were shown in this paper. The full analysis of this data can be found in [4].

Due to the monitoring and the appropriate data analysis it could be confirmed that the Monolithic Bridge performed well in the alpine environment. As a result it is planned to use the new bridge design more often.

## ACKNOWLEDGEMENTS

We want to thank the staff of ZT Eisner, especially DI Herbert Högler who designed the Monolithic Bridge, for the opportunity to monitor this unique structure. In addition we are grateful to the Austrian Industrial Research Promotion Fund (FFF) who partly funded the monitoring project.

## REFERENCES

1. Högler, H. and Lienhart, W., 'Integrales Brückenbauwerk zur Straßenverbreiterung und erste Deformationsmessungen mit faseroptische Sensoren', VDI Berichte 1757 (2003) 221-231.
2. Inaudi, D., Elamari, A., Pflug, L., Gisin, N., Breguet, J. and Vurpillot, S., 'Low-coherence deformation sensors for the monitoring of civil engineering structures', Sensors and Actuators 44 (1994) 125-130.
3. Lienhart, W., 'Experimental Investigation of the Performance of the SOFO Measurement System', Proceedings of 5<sup>th</sup> International Workshop on Structural Health Monitoring, Stanford (2005) 1131-1138.
4. Lienhart, W., 'Analysis of Inhomogeneous Structural Monitoring Data', Series 'Engineering Geodesy – TU Graz', Shaker Verlag, Aachen, Germany (2007).
5. Inaudi, D., Casanova, N., Vurpillot, S., Glisic, B., Kronenberg, P. and Lloret, S., 'Lessons learned in the use of fiber optic sensor for civil structural monitoring', Proceedings of 6<sup>th</sup> Intern. Workshop on Material Properties and Design, Present and Future of Health Monitoring, Weimar, Germany, September 2000 (2000) 79-92.
6. Welsch, W.M. and Heunecke, O., 'Models and Terminology for the Analysis of Geodetic Monitoring Observations', Proceedings of 10<sup>th</sup> international FIG-Symposium on Deformation Measurements, Orange, USA (2001) 390-412.
7. Cooper, M.A.R., 'Control Surveys in Civil Engineering', Nichols (1987).
8. Kälber, S. and Jäger R., 'Realisierung eines GPS-basierten Online Kontroll- und A-larmsystems (GOCA) und Diskussion adäquater geometrischer und systemanalytischer Ansätze zum online Monitoring im Talsperrenbereich', Proceedings of 2<sup>nd</sup> Mittweidaer Talsperrentag (2000) 73-88.
9. Jäger, R. and Bertges M., 'Integrierte Modellbildung zum permanenten Monitoring von Bauwerken und geotechnische Analogien', Schriftenreihe des DVW 46 (2004) 101-139.